Vol. 14(1): 160-178, January 2026 DOI: https://doi.org/10.23960/jsl.v14i1.1259

P-ISSN: 2339-0913
E-ISSN: 2549-5747

Jurnal Sylva Lestari

Journal homepage: https://sylvalestari.fp.unila.ac.id

Full Length Research Article

Mangrove Cover and Shoreline Changes Detection using Multi-Temporal Landsat Imagery and Digital Shoreline Analysis System (DSAS) in Labuhanbatu Regency, Indonesia

Samsuri[1,*], Anita Zaitunah[2], Nailatul Amaliah[2], Yohanes Budi Sulistioadi[3,4], Duryat[5]

[1] Laboratory of Forest Inventory, Faculty of Forestry, Universitas Sumatera Utara, Medan, Indonesia
[2] Laboratory of Remote Sensing, Faculty of Forestry, Universitas Sumatera Utara, Medan, Indonesia
[3] Laboratory of Climate, Soil and Water Conservation, Faculty of Forestry, Mulawarman University, Samarinda, Indonesia
[4] Graduate Program of Environmental Science, Mulawarman University, Samarinda, Indonesia
[5] Department of Forestry, Faculty of Agriculture, University of Lampung, Bandar Lampung, Indonesia
[*] Corresponding Author. E-mail address: samsuri@usu.ac.id

ARTICLE HISTORY:

Received: 29 August 2025
Peer review completed: 13 December 2025
Received in revised form: 19 January 2026
Accepted: 21 January 2026

KEYWORDS:

Abrasion
Change detection
Land cover
Mangrove
Shoreline

© 2026 The Authors. Published by the Department of Forestry, Faculty of Agriculture, University of Lampung. This is an open access article under the CC BY-NC license: https://creativecommons.org/licenses/by-nc/4.0/.

ABSTRACT

Understanding the dynamics of the relationship between shoreline change and mangrove forest cover change is important for a foundation in mangrove and coastal forest management. The study aimed to analyze multitemporal changes in mangrove cover and shoreline in coastal areas and to investigate the correlation between these changes from 2011 to 2024. The research used remote sensing data to derive mangrove cover changes and detect shoreline changes from Landsat images acquired in 2011, 2015, 2019, and 2024. Land cover changes were examined using the operational land imager sensor, bands 3 and 6 of Landsat 8 images and bands 2 and 5 of Landsat 5 images, and shoreline changes were measured using the digital shoreline analyses system (DSAS). The result showed a reduction of 580.07 ha (26.48%) in mangrove cover area over eight years (2011–2019), followed by an increase of about 1,931.59 ha (54.54%) in 2024. Low abrasion (0.01–108.41 m) and low accretion (0–106.78 m) per four-year interval dominate in shoreline change. However, the Pearson correlation showed a moderate but non-significant association between changes in mangrove cover and shoreline changes ($r = 0.307$, $p = 0.266$). These results demonstrate that the correlation between mangrove cover change and shoreline change is non-linear, suggesting that shoreline change is affected not only by mangrove change but also by various other factors, including sedimentation events. It indicates that additional factors, including geomorphological dynamics, significantly influence mangrove forest dynamics.

1. Introduction

Indonesia is an archipelago that sits between the Asian continent and Australia, as well as the Pacific and Indian Oceans. Indonesia is an archipelagic country with 99,093 km of coastline (BPS 2016). This coastline is a transition zone between land and sea that changes shape and location over time (Nath et al. 2021). Dense vegetation, especially mangroves, can protect land from storms, waves, abrasion, and tsunamis (Zaitunah et al. 2018). Coastal ecosystems are still under stress and disturbance from both natural and human activities, in any case (Lovelock and

Brown 2019), this results in changes to vegetation cover and coastal areas, either in the form of abrasion (i.e., erosion or loss of land) and accretion (i.e., sediment deposition or land expansion) of coastal areas.

The North Sumatra coast is one of the coastal areas experiencing pressures from human population growth and the expansion of oil palm plantations (Zaitunah 2019). It includes the coastal areas in Labuhanbatu regency, located in the eastern part of the province. It is important to understand the dynamics of coastal areas by measuring shoreline changes, which is necessary for managing them (Mishra et al. 2020). The coastal region, vital to state and community income, is under immense pressure from human activities such as settlements and industry, leading to significant changes (Lubis et al. 2017).

Detection and monitoring of shoreline changes are essential for assessing potential hazards in coastal areas (Armenio et al. 2019; Baig et al. 2020), as they are important considerations when making decisions and developing management strategies for coastal areas as soon as possible and as precisely as possible. In this regard, the remote sensing technology can provide fast and accurate information to support management strategies (Iskandar et al. 2024), to mitigate anthropogenic impact in coastal areas (Kennish 2022), and to make the best management decisions through the integration of biophysical and socio-economic data in coastal management (Arfan et al. 2023; Mishra et al. 2020). Land use patterns are influenced by socio-cultural conditions and economic factors, leading to changes in land use for economic activities, particularly in developing countries like Indonesia.

However, most previous studies focus primarily on periods of continuous mangrove loss and shoreline retreat (Goldberg et al. 2020). In contrast, long-term analyses that capture both degradation and recovery phases of mangrove ecosystems remain limited. Many other studies describe the spatial relationships between mangrove distribution and shoreline change, but do not statistically test their strength and significance over long time periods (Nguyen et al. 2015). Therefore, they cannot adequately illustrate the potential influence of other controlling factors, such as large-scale sediment accretion, hydrodynamic processes, and anthropogenic activities, because these factors have not been identified, particularly on sediment-dominated and muddy shorelines such as those along the east coast of Sumatra.

Furthermore, Landsat satellite observations before 2019 (about 27 years) revealed rapid mangrove expansion following extensive accretion events, which were rarely incorporated into mangrove shoreline studies (Macreadie et al. 2023; Zhai et al. 2019). The knowledge gap regarding whether mangrove recovery primarily drives shoreline accretion or, conversely, is a response to the geomorphological processes that initially created suitable substrate for mangrove formation is a question this study must address. Therefore, the non-linear relationship between mangrove cover change and shoreline dynamics is examined in a coastal mangrove ecosystem. Therefore, this study analyzes multitemporal changes in land use and land cover (LULC), particularly mangrove forests, and shoreline position in the coastal area of Labuhanbatu Regency, North Sumatra. This study also identifies changes in mangrove cover using Landsat imagery from 2011, 2015, 2019, and 2024; analyzes shoreline change rates using the Digital Shoreline Analysis System (DSAS); and evaluates the statistical relationship between changes in mangrove cover and shoreline dynamics. The findings are expected to contribute to a better understanding of non-linear mangrove–shoreline interactions and to provide scientific support for coastal management and mangrove restoration strategies in sediment-dominated tropical coastal environments.

2. Materials and Methods

2.1. Research Location

The research was conducted in the coastal area of Labuhanbatu Regency, North Sumatra Province, Indonesia (**Fig. 1**). Data analysis was conducted at the Forest Management Laboratory, Faculty of Forestry, Universitas Sumatera Utara. The data analysis stage for the image and map is shown in the flowchart (**Fig. 2**).

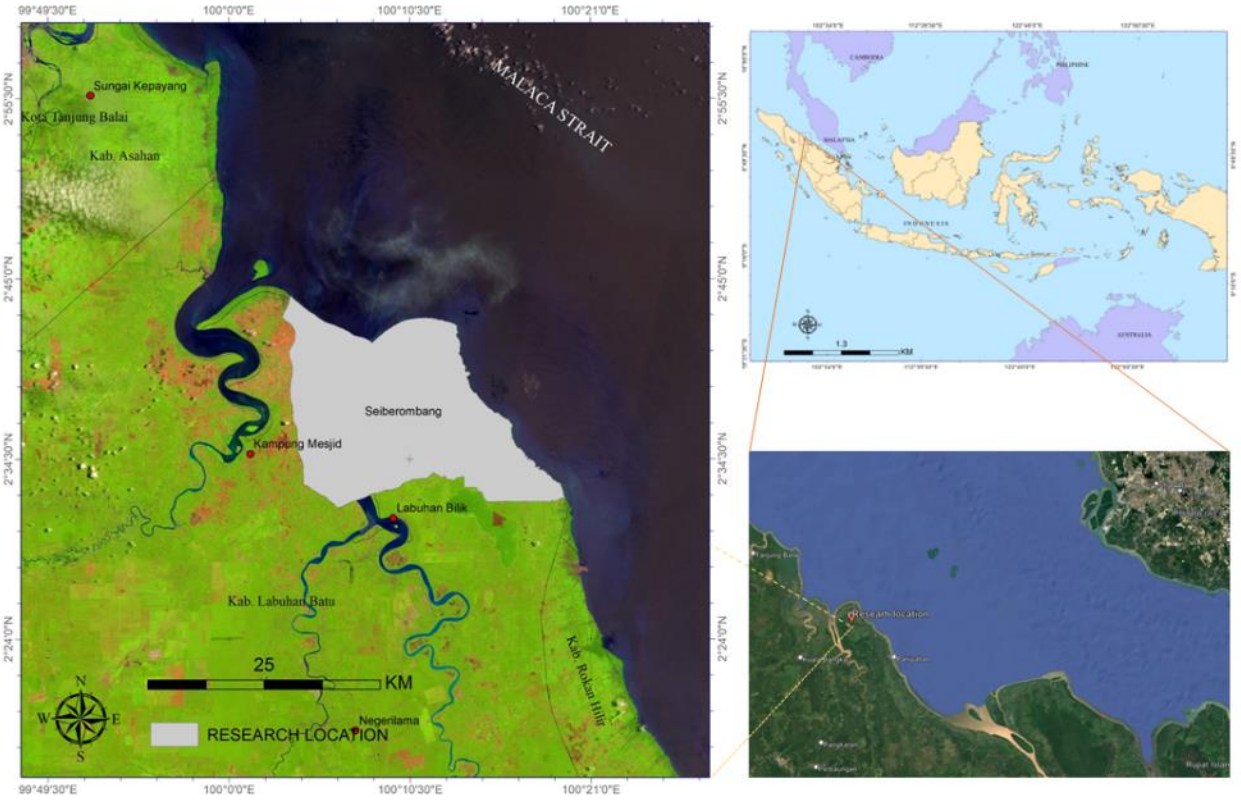

Fig. 1. Map of the research site in Labuhanbatu regency, North Sumatra Province, Indonesia.

2.2. Tools and Materials

The tools employed included data collection tools and data analysis tools. The data collection tools were a global positioning system (GPS), a digital camera, a tally sheet, and a roll meter. ArcGIS 10.8 and Er Mapper 7.0 were used to process and analyze satellite imagery data. The materials used were ground check data, Landsat images, and an administrative map.

2.3. Data Collection

Primary data were collected through on-site verification, while secondary data were obtained from government agencies (Geospatial Information Agency, Indonesia) and from Landsat Level 1 images from 2011, 2015, 2019, and 2024 (**Table 1**). Other Landsat images, such as those from Landsat 7 in 2011, were excluded because they contain a significant amount of cloud cover (more than 20%), making them unsuitable for optimal analysis. Additionally, the Landsat images were geometrically and radiometrically corrected and then cropped.

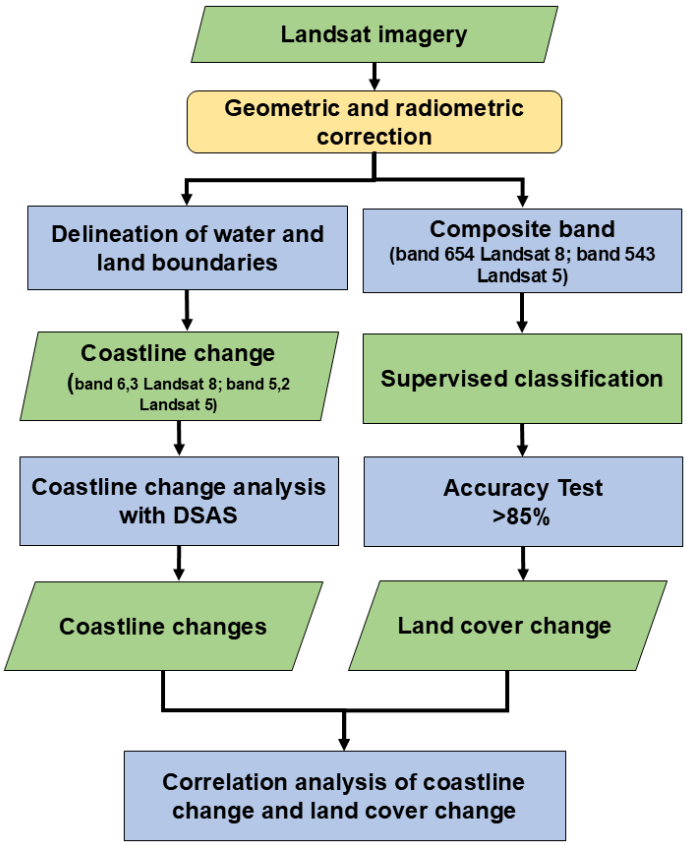

Fig. 2. Imagery and spatial analysis flowchart.

Table 1. Properties and date of acquisition were used in the research

Landsat type	Date acquisition	Time acquisition	Elevation	Azimuth
Landsat 8	2019-09-05	03:34:59.20	63.64187455	80.17286112
	2015-04-19	03:34:09.23	62.49412011	71.45895115
	2024-07-24	09:29:37.00	57.62996177	56.43202731
Landsat 5	2011-02-19	03:24:45.07	54.66628712	114.47696773

Geometric correction improves image accuracy by restoring pixel locations on Earth's surface, while radiometric correction adjusts pixel values influenced by atmospheric conditions. Image cropping focuses on boundaries and simplifies analysis. This study uses multi-temporal Landsat imagery, so radiometric correction is required. Images of higher quality (year 2015) are used as references for radiometric corrections. The PIF pixel values in the target and reference images were analyzed using simple linear regression for each spectral band, as recommended by Schott et al. (1988), which has become a reference in recent multi-temporal remote sensing studies (Canty and Nielsen 2019; Wu et al. 2018; Syariz et al. 2019). Multi-temporal Landsat imagery radiometric correction using the multiple date image normalization (MDIN) method based on pseudo-invariant features (PIF). Radiometric correction aims to correct pixel values to their true values and typically considers atmospheric disturbance factors as the main source of error (Zhu et al. 2015), since Landsat records exhibit varying radiometric interference. Objects that have not changed are deep water bodies, bare soil, and building roofs (Wu et al. 2018). This approach is widely used in coastal change analysis because it does not require field atmospheric data and is effective for long-term multi-temporal studies (Chen et al. 2022). The normalized images were

then used for shoreline extraction and analyzed using the digital shoreline analysis system (DSAS) to quantitatively calculate the direction and rate of coastal abrasion and accretion (Himmelstoss et al. 2018; Himmelstoss et al. 2021).

2.4. Data Analysis

2.4.1. Land cover of the coastal area

Three-band images (6, 5, 4) of Landsat 8 and (5, 4, 3) of Landsat 5 were composited to make the new composition easier to interpret. A composite band is a process of combining bands in an image to simplify remote sensing processing. The composite bands used to identify LULC classes were 6, 5, and 4 of Landsat 8 and 5, 4, and 3 of Landsat 5, because these bands have high reflectance values for vegetation, water, and bare land. Supervised classification is a process for obtaining various land classifications by characterizing classes using a known sample of pixels created within a training area. In this study, the maximum likelihood method was used in ArcGIS 10.8 because it can quantitatively assess spectral response variance and correlation when classifying unknown pixels. The accuracy test was conducted to determine the error rate in the sample area classification process by comparing satellite image classifications with field data. If the accuracy test value exceeds 85% of Kappa's accuracy, the results can be used.

2.4.2. Delineation of water and land boundaries

The determination of water and land boundaries was carried out using the ratio formula. Rationing is used to compare the brightness value of images. This ratio value can distinguish fine wetlands and detect different types of water bodies (Acharya et al. 2016; Jensen 1986). Brightness values are increasingly relevant in imaging functions and computer capabilities due to their utility, contextual relevance, and ease of normalization. The brightness value is very important for detecting shoreline changes because it enables more effective data measurement and analysis than the reflectivity value. For ease of measurement, high-contrast difference, change detection, and analysis, brightness values are preferred (Kumar and Mutanga 2017; Cheng et al. 2024), and they also improve accuracy (Li et al. 2020). Topographic conditions, shadows, or seasonal changes affect brightness values (BV), or the level of imaging brightness at a given location, as calculated using Equation 1.

$$\mathrm{BV}_{ijr} = \frac{\mathrm{BV}_{ijk}}{\mathrm{BV}_{ijl}} \quad (1)$$

where BV_{ijr} is the output ratio in row 'i' column 'j', BV_{ijk} is the BV at the exact location as the band 6, and BV_{ijl} is the BV in bands 3, 6.

The rationing process was performed using Er Mapper 7.0. The resulting rationing data were digitized to delineate water and land areas. To distinguish water and land areas in the rationing process, the processing used Landsat 8 imagery in bands 6 and 3, and Landsat 5 imagery in bands 5 and 2.

2.4.3. Calculation of coastline change

Shoreline change was calculated using the digital shoreline analysis system (DSAS) software (Baig et al. 2020; Himmelstoss et al. 2018; Sebat and Salloum 2018). The statistical method used to analyze the endpoint rate (EPR) is described by Baig et al. (2020) and Ghosh and Mistri (2021).

EPR calculates shoreline changes by dividing the distance between the oldest and most recent shorelines over a period of time (Baig et al. 2020). As a baseline, using the 2011 coastline; furthermore, comparing with the coastlines in 2015 and 2019, and comparing 2019 with 2024; and calculating the rate of coastline change. Field measurements and field examinations to validate the results of the calculation of shoreline changes, as well as to ensure the difference in position between land and sea. The classification of coastal erosion and accretion levels was performed using the K-Means algorithm on the rate of coastal change derived from DSAS for each transect. The number of clusters was set to 7 (K = 7), representing high abrasion, moderate abrasion, low abrasion, stable (0), low accretion, moderate accretion, and high accretion. The K-Means algorithm groups transects based on the similarity of the rate of coastline change, minimizing the Euclidean distance to the cluster center (centroid). The iteration process continues until cluster membership stabilizes.

The study calculated changes in coastline length using EPR and produced a map showing the magnitude of the shoreline change (y). Overlays of mangrove land-cover maps from different years produce a map of mangrove forest change (x). Every change from mangrove forests to non-mangroves is given a score of 1, and no change (i.e., mangroves remaining) is given a score of 0. The map of coastline change is overlaid with a map of mangrove forest change, enabling identification of coastal shifts and mangrove forest changes. Variables Y and X were then analyzed for correlation using Pearson's correlation analysis. Pearson's correlation coefficient was used to examine the relationship between LULC and coastline change, assuming a normal distribution of the data. The formula used is Equation 2 as follows.

$$r = \frac{\sum xy - \frac{\sum x - \sum y}{n}}{\sqrt{(\sum x^2 - \frac{(\sum x)^2}{n})(\sum y^2 - \frac{(\sum y)^2}{n})}} \quad (2)$$

where *r* is the correlation, *x* is the mangrove forest change value, y is the shoreline change, and *n* is the number of samples.

3. Results and Discussion

3.1. Results

3.1.1. LULC of the coastal area in 2011, 2015, 2019, and 2024

Based on 225 points of observation, eight land-cover types were identified in the field: water bodies, dry land forests, mangrove forests, built-up areas, bare land, coastal (beach), oil palm plantations, and shrubs. The accuracy value of the 2019 LULC classification results using the Kappa accuracy method is 89.07%. The accuracy results must meet the USGS requirements, specifically an interpretation accuracy of more than 85%. Land-cover maps for 2011, 2015, 2019, and 2024 in the coastal area of the Labuhanbatu Regency are shown in **Fig. 3**.

Table 2 shows that palm oil plantation cover increased the most from 2011 to 2019, followed by dryland forest, built-up area, and water bodies, while beach LULC experienced the largest reduction. The LULC category that underwent the most significant expansion in area from 2011 to 2019 was the built-up area at 71.56%, followed by dryland forest at 69.58%, oil palm plantations at 66.63%, and water bodies at 5.94%, while the LULC class that underwent the most significant decrease in area from 2011 to 2019 was the beach at 80.37%, followed by shrubs at 30.76%,

mangrove forest at 26.48%, and bare land at 18.51 %. The difference lies in LULC during the 2019–2024 period, with increases in mangrove forests (54.53%) and coastal areas (80.46%). On the other hand, dryland forests (22.13%) and oil palm plants experienced a slight decrease in area (0.45%).

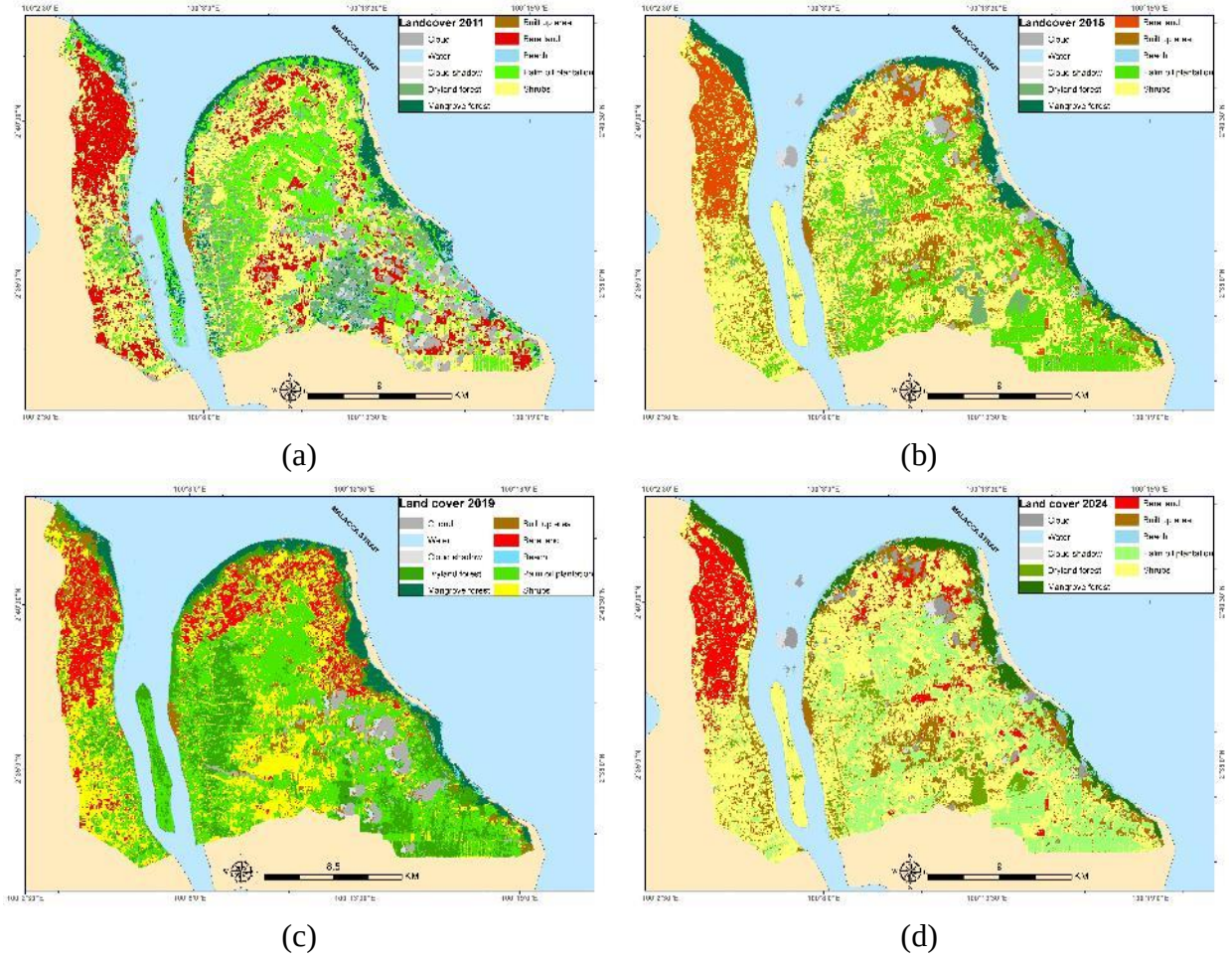

Fig. 3. LULC maps of the coastal area of Labuhanbatu Regency in: (a) 2011, (b) 2015, (c) 2019, and (d) 2024.

Table 2. LULC changes in the coastal area of Labuhanbatu Regency between 2011 and 2024

No	Landcover	2011-2015		2015-2019		2011-2019		2019-2024	
		(ha)	%	(ha)	%	(ha)	%	(ha)	%
1	Waterbody	97.47	2.04	186.78	3.83	284.25	5.94	104.27	2.02
2	Dryland forest	702.75	21.22	1,601.59	39.9	2,304.34	69.58	-1,017.53	-22.13
3	Mangrove	-186.73	-8.52	-393.34	-19.62	-580.07	-26.48	1,931.59	54.53
4	Built-up area	687.90	49.06	315.41	15.09	1,003.31	71.56	332.14	12.13
5	Bare land	-1,271.51	-27.65	420.57	12.64	-850.94	-18.51	387.58	9.37
6	Beach	-473.11	-19.77	-1,449.89	-75.53	-1,923.00	-80.37	1,933.86	80.46
7	Palm oil plantation	1,092.41	16.62	3,286.21	42.88	4,378.62	66.63	-48.94	-0.45
8	Shrubs	935.49	7.94	-4,560.44	-35.85	-3,624.94	-30.76	-3,625.53	-79.94

Notes : (+) increase; (-) decrease.

3.1.2. Changes in mangrove forest cover in 2011–2024

The study reveals that only one LULC, mangrove forest, is directly adjacent to the coastline and falls under the authority of the Indonesian Ministry of Forestry. This protected forest surrounds the coastal area of Labuhanbatu Regency. Other LULCs include water bodies, dryland forests,

built-up areas, bare land, oil palm plantations, beaches, and shrubs. **Table 3** presents changes in mangrove forest cover and percentage for 2011–2015, 2015–2019, and 2011–2019, while **Table 4** presents changes in the coastal area. The total coastal area in Labuhanbatu Regency is 39,546.59 ha. Based on **Table 4**, mangrove forest cover in the area declined from 2011 to 2019, with decreases of 8.52% from 2011 to 2015 and 19.62% from 2015 to 2019. Mangrove forest area increased by 0.24% between 2011 and 2015, while the largest increase occurred from 2019 to 2024 at 1,424.90 ha.

Table 3. Area and percentage of mangrove forest cover and non-mangrove forest in the coastal area of Labuanbatu Regency

No	LULC	2011		2015		2019		2024	
		(ha)	%	(ha)	%	(ha)	%	(ha)	%
1	Mangrove	2,191.01	5.54	2,004.28	5.07	1,610.94	4.07	3,542.53	8.97
2	Non-mangrove	37,454.28	94.71	37,542.31	94.93	37,935.65	95.93	36,004.05	91.03
3	Total	39,546.59	100.00	39,546.59	100.00	39,546.59	100.00	39,546.59	100.00

Table 4. Percentage of area changes of mangrove forest and non-mangrove forest in the coastal area of Labuhanbatu Regency

No	LULC change	2011-2015		2015-2019		2011-2019		2019-2024	
		(ha)	%	(ha)	%	(ha)	%	(ha)	%
1	Mangrove to non-forest	-186.73	-8.52	-393.34	-19.62	-580.07	-26.48	-227.33	-14.00
2	Non-forest to mangrove	88.03	0.24	393.34	1.05	481.37	1.29	1,424.90	3.95

3.1.3. Shoreline change in the eastern coastal Labuhanbatu Regency

Analysis of coastline changes identified changes over several periods (**Table 5**). Meanwhile, overlaying the map of coastal change with the map of changes in mangrove forest cover shows the positions of abrasion and accretion based on mangrove forest cover changes (**Table 6**). These data indicate that mangrove forests tend to promote accretion, or an increase in land area, whereas non-forested mangrove areas tend to trigger coastal abrasion.

Table 5. Changes in the extent of shoreline abrasion and accretion in the coastal area in 2011, 2015, 2019, and 2024

Period (year)	Abrasion (ha)	Accretion (ha)
2011–2015	367.68	520.45
2015–2019	214.72	387.88
2011–2019	296.12	491.73
2019–2024	16.82	1,710.90

Table 6. Overlay the results of LULC change and shoreline change in the coastal area

No	Landcover change	Area (ha)	Coastline change	Area (ha)
1	Mangrove – non mangrove	106.64	Abrasion	62.28
2	Mangrove – mangrove	210.10	Accretion	85.38
3	Mangrove – mangrove	123.25	Accretion	262.60
4	Mangrove – mangrove	367.71	Accretion	47.82
5	Non mangrove – mangrove	187.15	Accretion	8.66
6	Non mangrove – non mangrove	974.81	Abrasion	103.43

No	Landcover change	Area (ha)	Coastline change	Area (ha)
7	Mangrove – mangrove	348.16	Accretion	34.57
8	Mangrove – mangrove	363.65	Accretion	69.50
9	Non mangrove – non mangrove	1,086.62	Abrasion	43.38
10	Non mangrove – non mangrove	3,306.54	Accretion	46.92
11	Non mangrove – non mangrove	1,865.41	Accretion	196.78
12	Non mangrove – mangrove	181.32	Accretion	222.58
13	Non mangrove – mangrove	199.05	Accretion	13.94
14	Mangrove – non mangrove	30.94	Abrasion	11.68
15	Mangrove – non mangrove	64.07	Abrasion	76.28

3.1.4. Mangrove change and shoreline change correlation

The study analyzed the correlation between shoreline changes and changes in mangrove coverage in coastal areas using statistical tests. The Pearson correlation coefficient showed a moderate positive relationship, with a value near 0. However, the p-value was 0.266, indicating no significant effect of land-cover changes on shoreline changes (**Table 7**). The distribution of mangrove cover change and coastline is illustrated in **Fig. 4.**

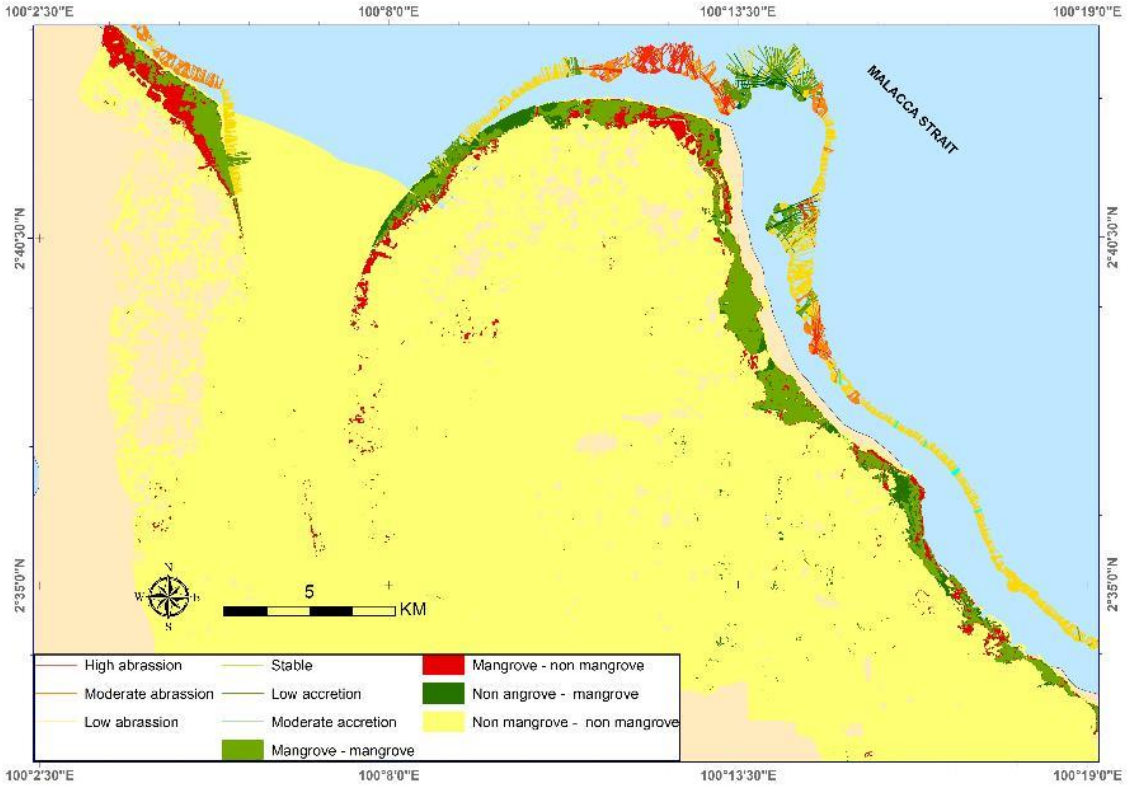

Fig. 4. Mangrove forest coverage change and shoreline change.

Table 7. Pearson correlation result analysis

Correlations		LULC change	Shoreline changed
LULC change	Pearson Correlation	1	0.307
	Sig. (2-tailed)		0.266
	N	15	15
Shoreline changed	Pearson Correlation	0.307	1
	Sig. (2-tailed)	0.266	
	N	15	15

3.2. Discussion

3.2.1. LULC change of the coastal area in 2011–2015

The largest increase in the percentage of LULC classes was in the built-up area, at 49.06% (**Fig. 5a**). This is consistent with data from the local government's central statistics agency, which reports that the population in the coastal area of Labuhanbatu Regency, mainly in the Panai Hilir District, increased from 35,839 in 2011 to 37,222 in 2019. This population increase will directly affect demand for residential areas because human activities (Zonkouan et al. 2022) require land for housing (Samsuri et al. 2022).

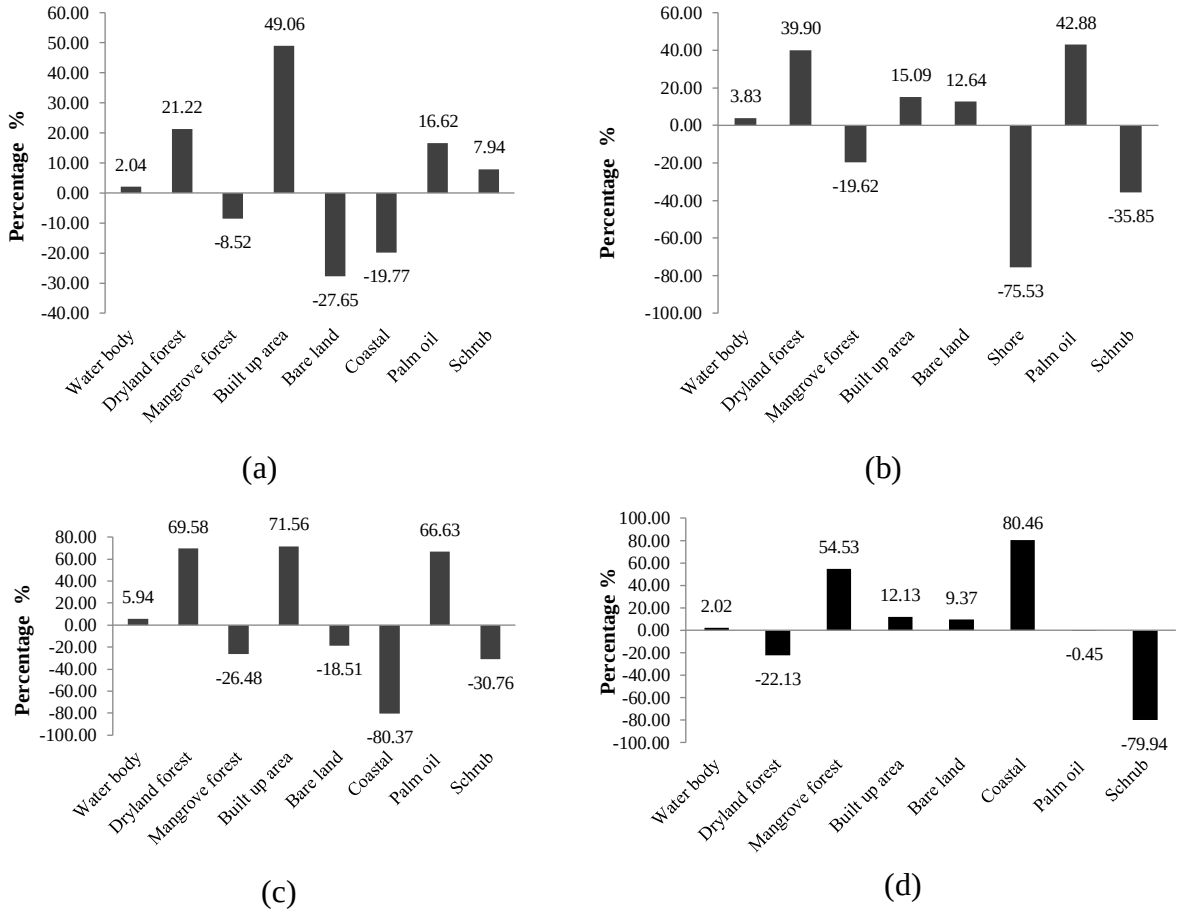

Fig. 5. LULC change percentage of the coastal area between: (a) 2011–2015, (b) 2015–2019, (c) 2011–2019, and (d) 2019–2024.

The largest decrease was in bare land, with 27.65%. LULC change between 2011 and 2015 (**Fig. 5a**) increased due to the conversion of areas into built-up areas and oil palm plantations, affecting mangrove areas (Eddy et al. 2017; Ibharim et al. 2024). Coconut and oil palm plantations have emerged as major drivers of mangrove loss, accounting for 18.0% and 4.7% of forest changes in Indonesia, respectively (Eddy et al. 2017; Himmelstoss et al. 2018). The trend is also observed in Malaysia, where oil palm plantations have encroached upon mangrove areas (Ibharim et al. 2024). Economic interests and a lack of awareness about the importance of the mangrove ecosystem often drive this conversion. Effective conservation requires recognizing mangroves' socio-economic importance and implementing policies that weigh conservation benefits against conversion costs (Acharya 2016).

3.2.2. LULC change of the coastal area in 2015–2019

Fig. 5b shows LULC changes from 2015-2019, with oil palm plantations experiencing the largest increase of 42.88% due to conversions from other LULC. According to Tatar et al. (2015), oil palm plantations can contribute to economic growth by creating jobs and generating income for the surrounding communities. The coastal areas experienced a 75.53% decrease due to accretion or sedimentation, a process driven by wave- and current-induced shoreline displacement into aquatic ecosystems (Anthony et al. 2015; Valderrama-Landeros et al. 2020). According to Angkotasan (2017), waves, wind, and tides are key drivers of abrasion and accretion, with waves influencing currents and sediment movement, thereby altering the shoreline.

3.2.3. LULC change of the coastal area in 2011–2024

The study shows that LULC changes between 2011 and 2019 increased or decreased (**Fig. 5c**), with the largest increase in built-up areas at 71.56%. This is due to population growth and increased demand for limited land resources, leading to competition for land use and changes in development to meet population needs and improve living standards. The coastal area experienced the largest decrease in LULC area, with 80.37%, due to accretion processes. This increase in land area is influenced by waves, ocean currents, and geological factors (Nikolakopoulos et al. 2019). Case studies from Popoh Beach, East Java, demonstrate significant accretion from 2015–2021, totaling 18.79 ha of land gain, with sand and clay sediment types dominating over abrasion processes despite an average wave energy of 1.5 kW/m per year (Miranda et al. 2023). Conversely, in Padang Pariaman, geological factors, including lithology, rock type, and topography, combined with climate variables such as rainfall and temperature, account for 62% of coastline change, with abrasion as the dominant process (Maulana and Prarikeslan 2024). Similarly, excessive accretion can harm coastal communities, ecosystems, and river mouths, as accretion processes occur in 60% of the Amapá Coastal Zone, affecting 14 of the 20 villages under observation and causing infrastructure damage and further saltwater incursion (Baia and Junior 2025).

Mangrove forests in Indonesia are being significantly reduced by human activities, including logging, primarily for aquaculture, plantations, agriculture, settlements, infrastructure development, and firewood (Cahyaningsih et al. 2022; Richards and Friess 2016). It aligns with the global situation that illegal logging and conversion, often carried out by surrounding communities, are causing significant damage to mangrove forests (Bhagarathi and DaSilva 2024). However, between 2019 and 2024, the area of mangrove forests increased by 1,931.59 ha. This increase was due to a significant shift from non-forest cover to mangrove forests (**Table 4**). This increase in area is also possible due to the existence of a reasonably wide accretion in 2024 of 1,710.90 ha (**Table 5**).

3.2.4. Changes in the shoreline in the coastal area

Two types of Landsat imagery, Landsat 5 and Landsat 8, are used at appropriate intervals to detect shoreline changes, with Landsat 8 band 6 particularly effective. When combined with bands 4 (red) and 5 (near-infrared), it is effective at identifying coastal ecosystems and their temporal changes. Likewise, bands 5 (shortwave infrared), 4 (near infrared), and 3 (red) in Landsat 5 imagery are also effective. The ratio of Landsat 5 band 2 and Landsat 8 band 3, combined with

Landsat 5 band 5 and Landsat 8 band 6, provides the most effective image ratio for extracting coastlines, especially on muddy beaches in mangrove forests (Figliomeni et al. 2023).

The study categorized coastline changes in 2011, 2015, 2019 (**Fig. 6**), and 2024 (**Fig. 7**) using image digitization results, revealing five classes: high abrasion, medium abrasion, low abrasion, medium accretion, and high accretion (**Table 8**).

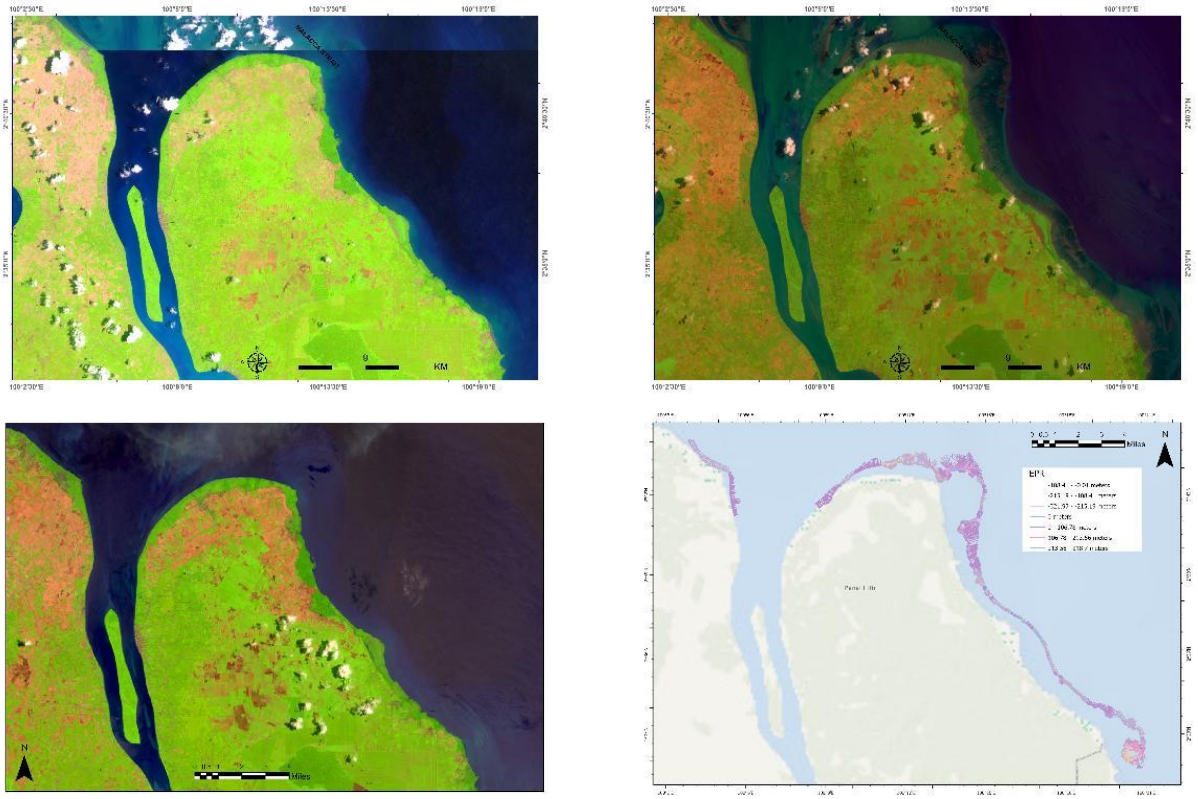

Fig. 6. Map of land coastline changes of the coastal area in Labuhanbatu Regency in 2011, 2015, and 2019.

Table 8. Classification of the rate of shoreline change in 2011, 2015, and 2019

No	Abrasion class	EPR (m/4 year)	Line length (m)	(%)
1	High abrasion	-321.97 – -215.19	4,406.23	0.49
2	Moderate abrasion	-215.19 – -108.41	22,940.55	2.53
3	Low abrasion	-108.41 – -0.01	414,022.24	45.60
4	Stable	0	30,737.45	3.39
5	Low accretion	0 – 106.78	390,050.65	42.96
7	Moderate accretion	106.78 – 213.56	45,880.54	5.05

The coastline changes from 2011 to 2019 were dominated by low abrasion and low accretion classes; meanwhile, in 2024, it is dominated by moderate abrasion and accretion **(Table 9).** The total amounted to 337.016.64 m (37.21%). The coastline changes slightly over 4 years, from -14.67 m to 31.17 m. This loss rate is lower than the erosion rate along the coast of Selangor, Malaysia, which is 50% (Daud et al. 2021). The activities of the surrounding community cause abrasion and accretion of the coast. The tides also influence it. Similarly, the Narrabeen embayment in Australia exhibits highly variable morphodynamic responses to moderate-to-high wave energy, with episodic storm events driving both erosion and accretion throughout the year

(Zhou et al. 2018). Prolonged exposure to large waves along the coast will result in both abrasion and accretion. High tides transport mud into deeper waters; if left uncontrolled, this can cause the shoreline to sink or erode through abrasion.

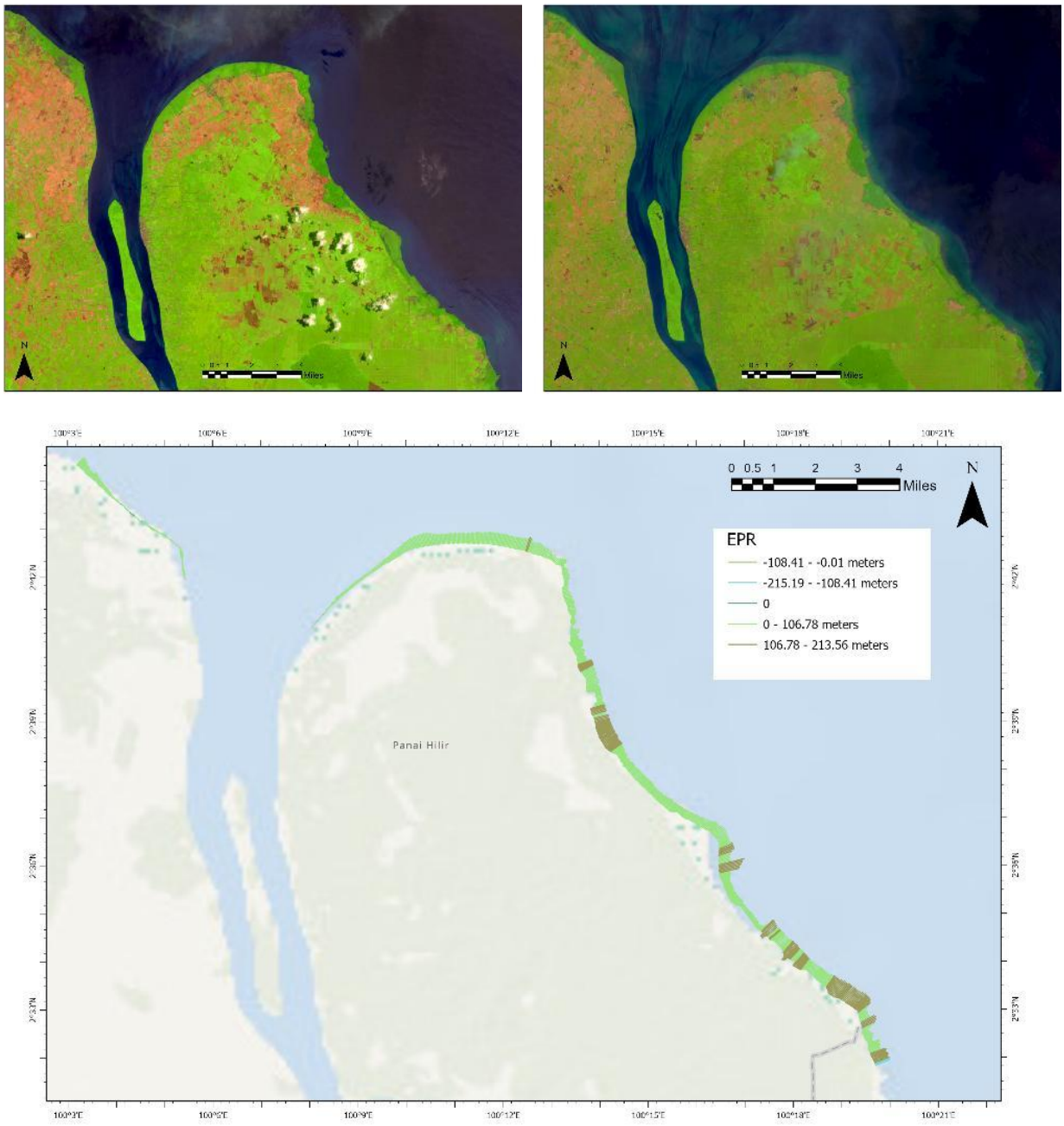

Fig. 7. Map of land coastline change of the coastal area in the Labuhanbatu Regency for 2019 to 2024.

The changes in the coastline from 2011 to 2019 were dominated by low abrasion and low accretion classes (**Table 8**); meanwhile, in 2024, they are dominated by moderate abrasion and accretion (**Table 9**). Along 414,022.24 m, coastal abrasion was low, ranging from -108.4 to -0.01 m per 4 years. Low abrasion, at -108.41 – -0.01 m/4 years, affects coastal areas, causing loss of residential land and livelihoods, and impacting the quality of life and the surrounding community's livelihoods. As is also the case on the east coast of Minahasa, coastal retreats of 23–43 m between 1980 and 2020 have reduced the area of residential land and damaged residential infrastructure

(Warouw et al. 2024); coastal abrasion in Central Java has reduced people's livelihoods (Riptanti et al. 2024). Coastal residents, such as fishermen, rely on natural resources that can be affected by activities such as industry, reclamation, settlement, and agriculture. These activities can increase pollution and massive erosion, exacerbate social conflict, reduce people's incomes, and erode the cultural aspects of coastal communities.

Table 9. Changes in the coastline in the period 2019–2024

No	Classification	EPR (m)	Line length (m)	%
1	High abrasion	-321.97 – -215.19	0	0.00
2	Moderate abrasion	-215.19 – -108.41	1,191.42	0.43
3	Low abrasion	-108.41 – -0.01	414.15	0.15
4	Stable	0	21.17	0.01
5	Low accretion	0 – 106.78	190,234.29	68.49
6	Moderate accretion	106.78 – 213.56	85,889.61	30.92
7	High abrasion	213.56 – 318.7	0	0.00

Low accretion and abrasion can harm ecosystems by increasing erosion, coastal change, and habitat loss for mangroves and wildlife, particularly on beaches with multiple river mouths. According to Chien and Tung (2018), wave-dominated coastal environments exhibit different accretion patterns, as demonstrated at Lach Van, Vietnam, where shoreline accretion occurs at ~10 m/yr on both sides of the river mouth due to sediment transport over the long coastal area.

3.2.5. Coastline changes and LULC changes relation

This study identified a moderately correlated relationship (**Table 7**) between changes in mangrove cover and shoreline change, involving anthropogenic factors indirectly driving the changes. The complex relationship between shoreline change and mangrove change is significant along the east coast of Labuhanbatu (Wan et al. 2019). A similar finding was observed in Takalar Regency, Indonesia, where a positive correlation between shoreline change and mangrove density was observed; however, the correlation was not statistically significant ($p > 0.05$). It suggests that other factors may have a greater impact (Inaku et al. 2020). Similarly, a study conducted in Rangsang Barat, Indonesia, also found that mangrove forest destruction was associated with changes in shoreline erosion and accretion rates. This situation emphasizes the importance of mangroves in coastal defense (Mubarak et al. 2020). A similar situation also occurred along the Pati coastline in Indonesia, where a moderate correlation ($R = 0.299$) was observed between changes in mangrove density and shoreline modification. Higher mangrove densities tend to cause accretion (Inaku et al. 2020). Therefore, in developing mangrove forest management strategies, one guideline is the condition of the mangrove forest habitat and shoreline dynamics.

4. Conclusions

The use of composite bands 3 and 6 of Landsat 8 and bands 2 and 5 of Landsat 5, as well as the digital shoreline analysis system (DSAS), provides a fairly good distinction between coastline and land cover changes in Labuhanbatu Regency, North Sumatra. The study found a non-linear pattern of mangrove dynamics, with a reduction in the extent of mangrove forests in the Labuhanbatu District, amounting to a 580.07 ha (26.48%) decrease from 2011–2019, followed by

an increase of about 1,351.52 ha in 2024. The coastline changes from 2011–2019 were dominated by low abrasion and low accretion classes; meanwhile, in 2024, it is dominated by moderate abrasion and accretion. Statistical analysis of Pearson correlation indicated a moderate but statistically non-significant relationship ($r = 0.307$, $p = 0.266$) between mangrove cover changes and shoreline dynamics, suggesting that other factors (e.g., waves, tides, human activities) may also influence coastal morphology. The existence of forest degradation and recovery events over a reasonably long period addresses the research gap in understanding the linear tidal relationship between changes in mangrove cover and coastlines. Research also shows that mangrove improvement is likely triggered by geomorphological processes rather than solely by shoreline accretion. From the perspective of forest management, this study emphasizes the need to integrate sedimentation dynamics processes in mangrove restoration and protection strategies.

Acknowledgments

The authors would like to thank the Lembaga Penelitian – Universitas Sumatera Utara (LP-USU) for funding this Collaboration Research with Higher Education University schema for 2022. The author also thanks Universitas Sumatera Utara for its support.

Author Contributions

S.: Conceptualization, Methodology, Data Curation, Writing – Review and Editing; A.Z.: Conceptualization, Methodology, Data Curation, Writing – Review and Editing; N.A.: Data Curation, Writing – Original Draft Preparation, Writing – Review and Editing, Visualization; Y.B.S.: Validation, Writing – Review and Editing; D.: Validation, Writing – Review and Editing.

Conflict of Interest

The authors declare no conflict of interest.

Declaration of Generative AI and AI-Assisted Technologies in the Manuscript Preparation

Not applicable.

References

Acharya, G. D. 2016. Life at the Margins: The Social, Economic and Ecological Importance of Mangroves. *Madera y Bosques* 8(1): 53–60. DOI: 10.21829/myb.2002.801291

Acharya, T. D., Lee, D. H., Yang, I. T., and Lee, J. K. 2016. Identification of Water Bodies in a Landsat 8 OLI Image Using a J48 Decision Tree. *Sensors* 16(7): 1075. DOI: 10.3390/s16071075

Angkotasan, A.M., Nurjaya, I.W., Natih, N.M. 2017. Analisis Perubahan Garis Pantai Di Pantai Barat Daya Pulau Ternate, Provinsi Maluku Utara. *Jurnal Teknologi Perikanan Dan Kelautan* 3(2): 11–22. DOI: 10.24319/jtpk.3.11-22

Anthony, E. J., Brunier, G., Besset, M., Goichot, M., Dussouillez, P., and Nguyen, V. L. 2015. Linking Rapid Erosion of the Mekong River Delta to Human Activities. *Scientific Reports* 5(1): 14745. DOI: 10.1038/srep14745

Arfan, A., Maru, R., Nyompa, S., Sukri, I., and Juanda, M. F. 2023. Analysis of Mangrove Density using NDVI and Macrobenthos Diversity in Ampekale Tourism Village, South Sulawesi, Indonesia. *Jurnal Sylva Lestari* 12(2): 230–241. DOI: 10.23960/jsl.v12i2.788

Armenio, E., Serio, F. D., Mossa, M., and Petrillo, A. F. 2019. Coastline Evolution Based on Statistical Analysis and Modelling. *Natural Hazards and Earth System Sciences* 19(9): 1937–1953. DOI: 10.5194/nhess-19-1937-2019

Badan Pusat Statistik (BPS). 2016. *Statistics of Marine and Coastal Resources*. BPS-Statistics, Indonesia.

Baia, M. M., and Junior, O. M. 2025. Morphological Changes in the Lower Estuarine Coastal Sector and Socio-Environmental Impacts—Amapá: Between 1992 and 2022. *Revista Brasileira de Geomorfologia* 26(2): 1–15. DOI: 10.20502/rbg.v26i2.2599

Baig, M. R. I., Ahmad, I. A., Shahfahad, Tayyab, M., and Rahman, A. 2020. Analysis of Shoreline Changes in Vishakhapatnam Coastal Tract of Andhra Pradesh, India: An Application of Digital Shoreline Analysis System (DSAS). *Annals of GIS* 26(4): 361–376. DOI: 10.1080/19475683.2020.1815839

Bhagarathi, L. K., and Da Silva, P. N. B. 2024. Impacts and Implications of Anthropogenic Activities on Mangrove Forests: A Review. *Magna Scientia Advanced Research and Reviews* 11(1): 040–059. DOI: 10.30574/msarr.2024.11.1.0074

Cahyaningsih, A. P., Deanova, A. K., Pristiawati, C. M., Ulumuddin, Y. I., Kusumaningrum, L., and Setyawan, A. D. 2022. Review: Causes and Impacts of Anthropogenic Activities on Mangrove Deforestation and Degradation in Indonesia. *International Journal of Bonorowo LANDS* 12(1): 12–22. DOI: 10.13057/bonorowo/w120102

Canty, M. J., and Nielsen, A. A. 2019. *Radiometric Normalization of Multitemporal Satellite Imagery*. Springer, New York.Chen, D., Wang, Y., Shen, Z., Liao, J., Chen, J., Sun, S. 2022. Long Time-Series Mapping and Change Detection of Coastal Zone Land Use Based on Google Earth Engine and Multi-Source Data Fusion. *Remote Sensing* 14(1): 1. DOI: 10.3390/rs14010001

Cheng, G., Huang, Y., Li, X., Lyu, S., Xu, Z., Zhao, H., Zhao, Q., Xiang, S. 2024. Change Detection Methods for Remote Sensing in the Last Decade: A Comprehensive Review. *Remote Sensing* 16(13): 2355. DOI: 10.3390/rs16132355

Chien, N. Q., and Tung, T. T. 2018. Recent Sedimentation of a Mesotidal Wave-Dominated River Mouth: Lach Van, Vietnam. *Journal of Coastal Research* 81(1): 50–56. DOI: 10.2112/SI81-007.1

Daud, S., Milow, P., and Zakaria, R. M. 2021. Analysis of Shoreline Change Trends and Adaptation of Selangor Coastline Using Landsat Satellite Data. *Journal of the Indian Society of Remote Sensing* 49(1): 1869–1878. DOI: 10.1007/s12524-020-01218-0

Eddy, S., Iskandar, K., Ridho, M. R., and Mulyana, A. 2017. Land Cover Changes in the Air Telang Protected Forest, South Sumatra, Indonesia (1989–2013). *Biodiversitas* 18(4): 1538–1545. DOI: 10.13057/biodiv/d180432

Fela, W., Dwight, R., and Julianus, S. 2024. Study of the Impact of Coastline Changes on Coastal Settlement Areas along the East Coast of Minahasa. *Journal of Research and Community Service* 5(2): 203–212. DOI: 10.59188/devotion.v5i2.68

Figliomeni, F. G., Guastaferro, F., Parente, C., and Vallario, A. 2023. A Proposal for Automatic Coastline Extraction from Landsat 8 OLI Images Combining Modified Optimum Index Factor (MOIF) and K-Means. *Remote Sensing* 15(12): 3181. DOI: 10.3390/rs15123181

Ghosh, S., and Mistri, B. 2021. Delineating the Influence of Erosion and Accretion to Identify the Vulnerable Zone of Embankment Breaching in Gosaba Island, South 24 Parganas, West Bengal, India. *Journal of the Indian Society of Remote Sensing* 49(10): 2559–2574. DOI: 10.1007/s12524-021-01409-3

Goldberg, L., Lagomasino, D., Thomas, N., and Fatoyinbo, T. 2020. Global Declines in Human-Driven Mangrove Loss. *Global Change Biology* 26(10): 5844–5855. DOI: 10.1111/gcb.15275

Himmelstoss, E. A., Henderson, R. E., Kratzmann, M. G., and Farris, A. S. 2021. *Digital Shoreline Analysis System (DSAS) Version 5.1 User Guide*. Geological Survey, United States.

Himmelstoss, E. A., Henderson, R. E., Kratzmann, M. G., and Farris, A. S. 2018. *Digital Shoreline Analysis System (DSAS) Version 5.0 User Guide*. Geological Survey Open-File Report 2018–1179, United States.

Ibharim, Asyikin, N., Roslani, M. A., and Mustapha, M. A. 2024. Mangrove Dynamics Evaluation at Matang Mangrove Forest Reserve using Multi-Temporal Satellite Imageries. *Built Environment* 21(1): 1–15. DOI: 10.24191/bej.v21i1.250

Inaku, D. F., Nurdin, N., and Satari, D. Y. 2020. The Dynamics of Shoreline Changes Concerning the Existence of Mangrove in Takalar Regency. *IOP Conference Series: Earth and Environmental Science* 575(1): 012215. DOI: 10.1088/1755-1315/575/1/012215

Iskandar, B., Saidah, Kurnia, A. A., Jauhari, A., and Zannah, F. 2024. Modeling Land Cover Change using MOLUSCE in Kahayan Tengah Forest Management Unit, Kalimantan Tengah. *Jurnal Sylva Lestari* 12(2): 242–257. DOI: 10.23960/jsl.v12i2.865

Jensen, J. R. 1986. *Introductory Digital Image Processing: A Remote Sensing Perspective*. Prentice Hall, New Jersey.

Kennish, M. J. 2022. Management Strategies to Mitigate Anthropogenic Impacts in Estuarine and Coastal Marine Environments: A Review. *Open Journal of Ecology* 12(10): 667–688. DOI: 10.4236/oje.2022.1210038

Kumar, L., and Mutanga, O. 2017. Remote Sensing of Above-Ground Biomass. *Remote Sensing* 9(9): 935. DOI: 10.3390/rs9090935

Li, Z., Jia, Z., Liu, L., Yang, J., and Kasabov, N. 2020. A Method to Improve the Accuracy of SAR Image Change Detection using an Image Enhancement Method. *ISPRS Journal of Photogrammetry and Remote Sensing* 163(4): 137–151. DOI: 10.1016/j.isprsjprs.2020.03.002

Lubis, D. P., Pinem, M., and Simanjuntak, M. A. N. 2017. Analisis Perubahan Garis Pantai dengan Menggunakan Citra Penginderaan Jauh (Studi Kasus di Kecamatan Talawi Kabupaten Batubara). *Jurnal Geografi* 9(1): 21–31. DOI: 10.24114/jg.v9i1.6044

Lovelock, C. E., and Brown, B. M. 2019. Land Tenure Considerations Are Key to Successful Mangrove Restoration. *Nature Ecology and Evolution* 3(8): 1135–1137. DOI: 10.1038/s41559-019-0942-y

Maulana, I., Prarikeslan, W. 2024. The Influence of Geological Factors and Climate Change on Coastal Abrasion in Padang Pariaman Regency. *AL-DYAS* 3 (3): 974-885. DOI: 10.58578/aldyas.v3i3.3531

Miranda, N. A., Bintoro, R. S., and Prasita, V. D. 2023. The Pattern of Coastline Changes and Wave Modelling around the Expansion of PPI Popoh Tulung Agung, East Java. *Maritime Technology and Research* 5(4): 262926. DOI: 10.33175/mtr.2023.262926

Thakur, S., Mondal, I., Ghosh, P. B., Das, P., and De, T. K. 2020. A Review of the Application of Multispectral Remote Sensing in the Study of Mangrove Ecosystems with Special Emphasis on Image Processing Techniques. *Spatial Information Research* 28(1): 39–52. DOI: 10.1007/s41324-019-00268-y

Mubarak, N. A., Badrun, Y., and Syahputra, R. F. 2020. Relationship of Coastline and Mangrove Area in West Rangsang, Indonesia. *Journal of Southwest Jiaotong University* 55(5): 1–10. DOI: 10.35741/issn.0258-2724.55.5.20

Nath, A., Koley, B., Saraswati, S., Bhatta, B., and Ray, B. C. 2021. Shoreline Change and Its Impact on Land Use Pattern and Vice Versa: A Critical Analysis in and around Digha Area between 2000 and 2018 using Geospatial Techniques. *Pakistan Journal of Science and Technology* 29(1): 331–348. DOI: 10.47836/pjst.29.1.19

Nikolakopoulos, K., Kyriou, A., Koukouvelas, I., Zygouri, V., and Apostolopoulos, D. 2019. Combination of Aerial, Satellite, and UAV Photogrammetry for Mapping the Diachronic Coastline Evolution: The Case of Lefkada Island. *ISPRS International Journal of Geo-Information* 8(11): 489. DOI: 10.3390/ijgi8110489

Nguyen, H. H., McAlpine, C., and Pullar, D. 2015. Drivers of Coastal Shoreline Change: Case Study of Hon Dat Coast, Kien Giang, Vietnam. *Environmental Management* 55: 1093–1108. DOI: 10.1007/s00267-015-0455-7

Richards, D. R., and Friess, D. A. 2016. Rates and Drivers of Mangrove Deforestation in Southeast Asia, 2000–2012. *Proceedings of the National Academy of Sciences of the United States of America* 113(2): 344–349. DOI: 10.1073/pnas.1510272113

Riptanti, E. W., Harisudin, M., Kusnandar, Khomah, I., Setyowati, N., Qonita, A., and Gayatri, S. 2024. The Effect of Abrasion on the Resilience of Fishermen and Fish Farmer Livelihoods on the North Coast of Central Java. *Edelweiss Applied Science and Technology* 8(6): 1882–1894. DOI: 10.55214/25768484.v8i6.2354

Rosentreter, J. A., Laruelle, G. G., Bange, H. W., Bianchi, T. S., Busecke, J. J., Cai, W. J., Eyre, B. D., Forbrich, I., Kwon, E. Y., Maavara, T., Moosdorf, N., Najjar, R. G., Sarma, V. V. S. S., Dam, B. V., and Regnier, P. 2023. Coastal Vegetation and Estuaries Are Collectively a Greenhouse Gas Sink. *Nature Climate Change* 13(6): 579–587. DOI: 10.1038/s41558-023-01682-9

Samsuri., Zaitunah, A., and Pasaribu, D. 2022. Lands Cover Dynamics of Siais Lake Catchment Area, Tapanuli Selatan District, Indonesia. *IOP Conference Series: Earth and Environmental Science* 1116: 012084. DOI: 10.1088/1755-1315/1116/1/012084

Sebat, M., and Salloum, J. 2018. Estimate the Rate of Shoreline Change using the Statistical Analysis Technique (EPR). *Journal Business & IT* 8(1): 59–65. DOI: 10.14311/bit.2018.01.07

Singh, A. 1989. Review Article: Digital Change Detection Techniques Using Remotely Sensed Data. *International Journal of Remote Sensing* 10(6): 989–1003. DOI: 10.1080/01431168908903939

Syariz, M. A., Lin, B. Y., Denaro, L. G., Jaelani, M., Nguyen, M. V., Lin, C. 2019. Spectral-Consistent Relative Radiometric Normalization for Multitemporal Landsat 8 Imagery. *ISPRS Journal of Photogrammetry and Remote Sensing* 147: 56–64. DOI: 10.1016/j.isprsjprs.2018.11.007

Tatar, S., Saadatseresht, N., Arefi, M., Hadavand, H., and Ahmad. 2015. A New Object-Based Framework to Detect Shadows in High-Resolution Satellite Imagery over Urban Areas. *ISPRS Archives of the Photogrammetry, Remote Sensing and Spatial Information Sciences* XL-1/W5: 713–718. DOI: 10.5194/isprsarchives-xl-1-w5-713-2015

Valderrama-Landeros, L. H., Blanco y Correa, M., Flores-Verdugo, F., Álvarez-Sánchez, L. F., and Flores-de-Santiago, F. 2020. Spatiotemporal Shoreline Dynamics of Marismas

Nacionales, Pacific Coast of Mexico, Based on a Remote Sensing and GIS Mapping Approach. *Environmental Monitoring and Assessment* 192(2): 123. DOI: 10.1007/s10661-020-8094-8

Wan, L., Zhang, H., Lin, G., and Lin, H. 2019. A Small-Patched Convolutional Neural Network for Mangrove Mapping at the Species Level using a High-Resolution Remote-Sensing Image. *Annals of GIS* 25(1): 45–55. DOI: 10.1080/19475683.2018.1564791

Wu, W., Sun, X., Wang, X., Fan, J., Luo, J., Shen, Y., and Yang, Y. 2018. A Long Time-Series Radiometric Normalization Method for Landsat Images. *Sensors* 18(12): 4505. DOI: 10.3390/s18124505

Zaitunah, A., Thoha, A. S., Samsuri, and Siregar, K. 2019. Analysis of Coastal Vegetation Density Changes of Langkat Regency, North Sumatera, Indonesia. *IOP Conference Series: Earth and Environmental Science* 374(1): 012042. DOI: 10.1088/1755-1315/374/1/012042

Zaitunah, A., Samsuri, Slamet, B. 2018. Analysis of Greenbelt in Sibolga for Tsunami Mitigation. *IOP Conference Series: Earth and Environmental Science* 166 (1): 012028. DOI 10.1088/1755-1315/166/1/012028

Zhai, L., Zhang, B., Roy, S. S., Fuller, D. O., and Sternberg, L. S. L. 2019. Remote Sensing of Unhelpful Resilience to Sea Level Rise Caused by Mangrove Expansion: A Case Study of Islands in Florida Bay, USA. *Ecological Indicators* 97: 51–58. DOI: 10.1016/j.ecolind.2018.09.063

Zhou, Y., Feng, X., Guan, W., and Feng, W. 2018. Characteristics of Beach Erosion in Headland Bays Due to Wave Action: Taking the Narrabeen Beach in Australia as an Example. *Chinese Science Bulletin* 64(2): 223–233. DOI: 10.1360/n972018-00376

Zhu, Z., Woodcock, C. E., Holden, C., and Yang, Z. 2015. Generating Synthetic Landsat Images Based on All Available Landsat Data: Predicting Landsat Surface Reflectance at Any Given Time. *Remote Sensing of Environment* 162(2): 67–83. DOI: 10.1016/j.rse.2015.02.009